OL | Organic Letters

pubs.acs.org/OrgLett Letter

Structural Design and Synthesis of Bimodal PNA That Simultaneously Binds Two Complementary DNAs To Form Fused Double Duplexes

Manoj Kumar Gupta, Bharath Raj Madhanagopal, Dhrubajyoti Datta, and Krishna N. Ganesh*

Cite This: https://dx.doi.org/10.1021/acs.orglett.0c01950 Read Online

ACCESS | Metrics & More | Article Recommendations | Supporting Information

ABSTRACT: Bimodal PNAs are new PNA constructs designed to bind two different cDNA sequences synchronously to form double duplexes. They are synthesized on solid phase using sequential coupling and click reaction to introduce a second base in each monomer at C_α via alkyltriazole linker. The ternary bimodal PNA:DNA complexes show stability higher than that of individual duplexes. Bimodal PNAs are appropriate to create higher-order fused nucleic acid assemblies.

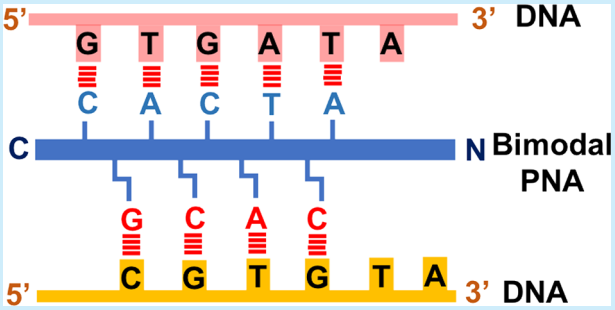

Peptide nucleic acids (PNA) are designed acyclic analogues of DNA endowed with an ability to recognize and bind complementary DNA/RNA sequences to form PNA:DNA and PNA:RNA duplexes.[1] The achiral PNA backbone with repeating units of aminoethylglycine (*aeg*) has nucleobases (A/T/C/G) connected via tertiary amide group (Figure 1a).[2] The structural geometry of *aeg* backbone in PNA ensures matching of the interbase distance in PNA with that of adjacent bases on the sugar−phosphate backbone of DNA/RNA,[3] leading to sequence-specific complementary base pairing between the PNA and the DNA/RNA complements (Figure 1b). PNA:DNA duplexes have strong binding and superior stability, compared to that of natural DNA:DNA duplexes.[4] This, along with unique strand invasion properties,[5] has allowed PNA to be used for several biotechnological applications in diagnostics[6] and antisense therapeutics.[7] The simplicity of PNA construct provides abundant opportunities for rational design of its structure to improve its properties[8] and cellular uptake.[9,10]

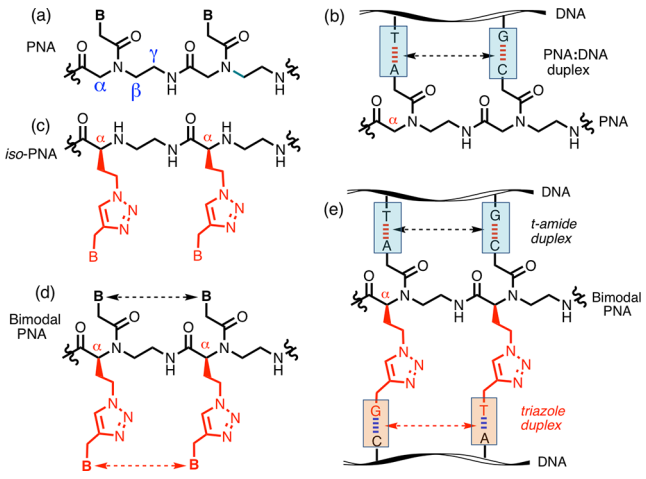

Figure 1. Structures of (a) *aeg*-PNA, (b) PNA:DNA duplex, (c) *iso*-PNA, (d) bimodal PNA (*bm*-PNA), and (e) bimodal PNA double duplex. B = T/A/G/C.

Substitutions on *aeg* backbone at C_α, C_β, and C_γ does not seriously impair the hybridization with cDNA/cRNA and, depending on the nature of substitution, PNAs acquire additional functions.[10,11] This manuscript describes the design of *iso*-PNA (Figure 1c) carrying nucleobases (A/G/C/T) on side chain at C_α linked through a triazole ring, instead of t-amide link. The interbase distance in *iso*-PNA is similar to that in original PNA and can be structurally fused with original PNA (Figure 1a) to generate "bimodal PNA" composed of two faces (Figure 1d). This equips a single PNA strand to recognize and concurrently bind two different DNA strands to produce double duplexes (Figure 1e) with a common PNA backbone.

Synthetic "Janus bases" known in literature recognize two natural bases, one from each face[12] and PNAs composed from such synthetic bases have innovative applications.[13] The

Received: June 10, 2020

https://dx.doi.org/10.1021/acs.orglett.0c01950
Org. Lett. XXXX, XXX, XXX−XXX

bimodal PNA "*bm*-PNA" (Figure 1d) described here are conceptually different with PNA backbone itself acquiring Janus character. *bm*-PNA is designed to bind cDNA/RNA/PNA as single strands or two strands simultaneously through canonical base pairing. It is demonstrated that *bm*-PNA forms double duplexes by simultaneous binding of two complementary DNA strands (Figure 1e) and the stability of the DNA:*bm*-PNA:DNA ternary complex is enhanced over that of isolated duplexes.

The target *iso*-PNA **1** and *bm*-PNA **2** (Figure 2) have nucleobases attached to $C_\alpha(S)$ of each glycyl component on

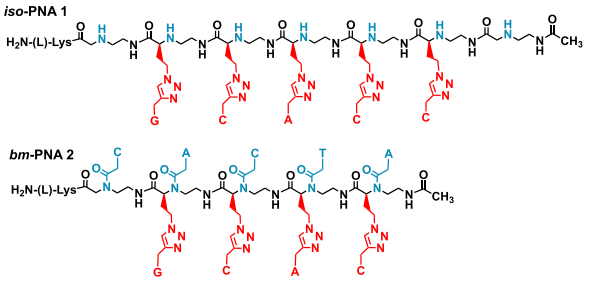

Figure 2. Structures of *iso*-PNA **1** and *bm*-PNA **2**.

aeg backbone through an ethyl triazole spacer (Figure 2). In *bm*-PNA **2** this is in addition to the standard t-amide linked nucleobases as in PNA. The triazole side chain at C_α design was chosen more due to ease of synthesis than any structural or functional considerations. *iso*-PNA **1** (Figure 2) bearing only nucleobases anchored on C_α side chain through triazole was used to test the ability of this new PNA analogue for base pairing with cDNA. The monomers **1**-**4** possessing C_α (*S*)-ethylazido side chain for subsequent click reaction were synthesized from easily available L-glutamine through intermediate steps via compounds **5**−**10** (Scheme 1). The monomers **11** (**B** = $C^{Cbz}/A^{Cbz}/G^{iBu}$) needed for assembling *iso*-PNA **1** were synthesized from azide **12** and base propynes **14**−**16** by click chemistry. The bimodal PNA monomer **17** having 2 bases per *aeg* unit was made by coupling **1** with **15**. The *aeg*-PNA-C monomer **18** was made by standard procedures.[14]

bm-PNA **2** with mixed sequence of five bases on t-amide side and four bases on triazole side was assembled by solid-phase synthesis on MBHA resin (Scheme 2), using well established protocols.[14] The first coupling on resin was done with standard PNA monomer **18** to avoid possible steric effects with modified monomers. Each coupling of C_α-ethylazido PNA monomers (**1**−**3**) on resin was followed by click reaction with appropriate base propynes (**14**−**16**). At an intermediate step, the preclicked bimodal PNA monomer **17** having T at the t-amide side and A on the triazole side was used to test strategy for future development of a general approach for synthesis of any mixed *bm*-PNA oligomers. The *iso*-PNA **1** was similarly synthesized on solid phase using monomers **11** (**B** = $C^{Cbz}/A^{Cbz}/G^{iBu}$). After the solid-phase synthesis, the resin bound *iso*-PNA **1** and *bm*-PNA **2** product oligomers were deprotected and cleaved from the resin, purified by reverse-phase HPLC and characterized by MALDI-TOF spectra (see the Supporting Information).

The successful formation of antiparallel PNA:DNA triazole duplexes from *iso*-PNA **1** and *bm*-PNA **2** (Figures 3A−E) was shown by sigmoidal transitions observed in a temperature−UV absorbance plot[14,15] (see Figure 4). The melting point (T_m)

Scheme 1. Structures of Monomers 1−4 and Their Synthesis

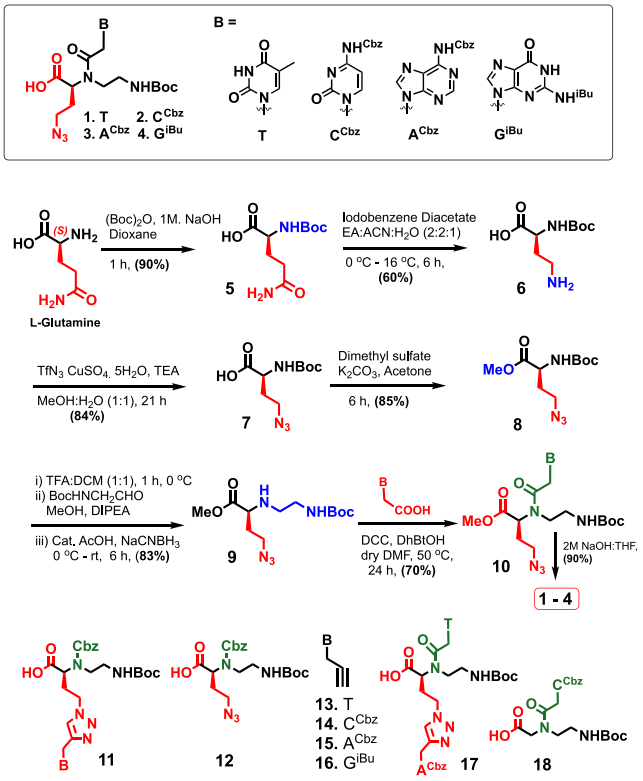

Scheme 2. Solid-Phase Synthesis of Bimodal PNA *bm*-PNA 2[a]

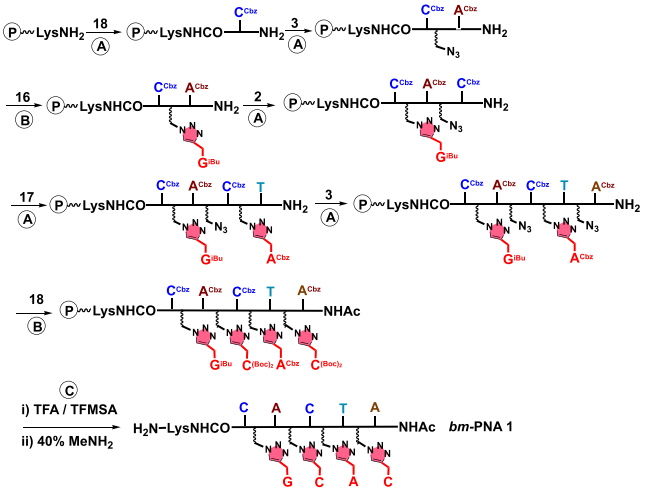

[a]Ⓐ *Monomer coupling*: (A/T/G/C; 3 equiv), dry DMF (500 μL) HOBt (3 equiv), HBTU (3 equiv), and DIPEA (3 equiv); Ⓑ *Click reaction*: resin (10 mg) in dry DMF:pyridine (1:1), alkyne (9 mg, 6 equiv), CuI (12 mg, 18 equiv), ascorbic acid (3 mg, 5 equiv), DIPEA (12 μL); and Ⓒ *Cleavage*: resin 10 mg, thioanisole (20 μL), 1,2-ethanedithiol (8 μL), TFA (200 μL), TFMSA (16 μL). Compound numbers at each step are taken from Scheme 2. For details regarding the reaction procedures, see the Supporting Information.

values extracted from the peak in the first derivative curves are shown in Figure 5. The *iso*-PNA **1**:DNA **1** duplex (Figure 3A) showed T_m of 42.8 °C, just for a 5-mer duplex (Figure 5A). Since it has cationic amino backbone, it is possible that it can also bind anionic DNA due to electrostatic interactions. To

https://dx.doi.org/10.1021/acs.orglett.0c01950
Org. Lett. XXXX, XXX, XXX−XXX

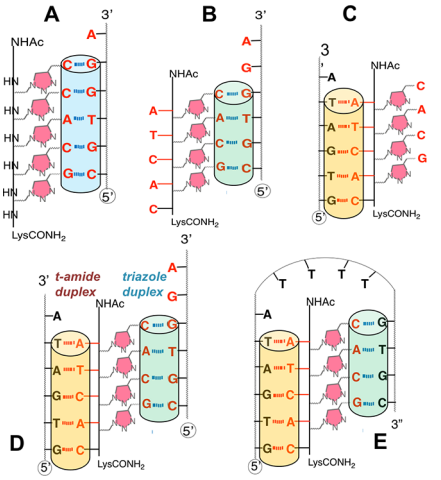

Figure 3. *iso*-PNA **1** and *bm*-PNA **2** duplexes: (A) *iso*-PNA **1**: DNA **1**; (B) *bm*-PNA **2**:DNA **1**; (C) DNA **2**:*bm*-PNA **2**; (D) DNA **2**:*bm*-PNA **1**:DNA **2** open double duplex and (E) DNA $\mathbf{3}_{hp}$:*bm*-PNA **2** hairpin double duplexes.

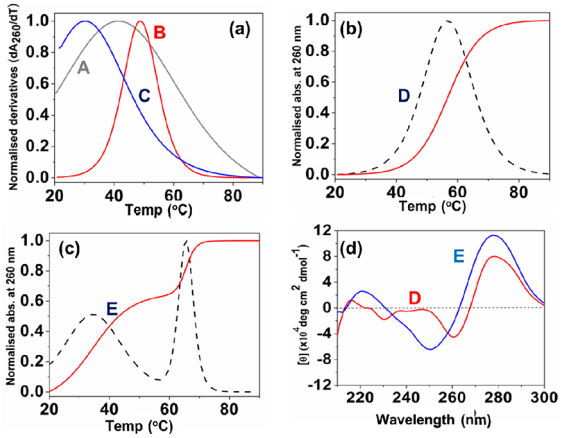

Figure 4. UV-melting plots and CD of duplexes. (a) **A**, *iso*-PNA **1**:DNA **1**; **B** *bm*-PNA **2**:DNA **1**; and **C** DNA **2**:*bm*-PNA **2**. (b) **D**, DNA **2**:*bm*-PNA **2**: DNA **1** and (c) **E** DNA $\mathbf{3}_{hp}$:*bm*-**PNA 2** (red line represents normalized melting curves and black dashed line represents first derivative plots). (d) CD profiles of duplexes **D** and **E**.

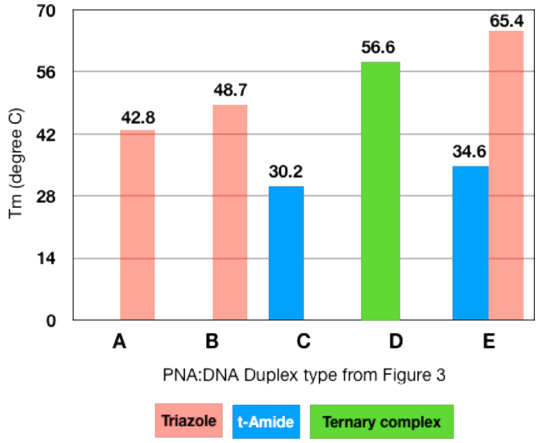

Figure 5. T_ms for various bimodal PNA:DNA duplexes and double duplexes, **A**–**E** correspond to complexes as in Figure 3. Values accurate to ±1.0 °C. *iso*-PNA **1**:DNA **1m** T_m = 24.7 °C, Mismatch DNA sequence: DNA **1m** = 5′-CG<u>C</u>GGA-3′.

test the sequence specificity of *iso*-PNA **1** binding to DNA **1**, its complementation was done with DNA **1m** (see legend in Figure 5) to yield duplex *iso*-PNA **1**:DNA **1m**, which has a C-T mismatch and exhibited a significantly lower T_m (24.7 °C). This suggests that *iso*-PNA **1**:DNA **2** duplex arises from specific base pairing and not mere electrostatic interactions.

The *bm*-PNA **2** formed corresponding triazole duplex *bm*-PNA **2**:DNA **1** (Figure 3B) with T_m of 48.7 °C (Figure 5B) that is slightly higher than that of *iso*-PNA **1**:DNA **1** triazole duplex. *bm*-PNA **2** also gave t-amide face duplex DNA **2**:*bm*-PNA **2** (Figure 3C) with T_m = 30.2 °C (Figure 5C), which is lower than that of its triazole duplex. Thus, the designed *bm*-PNA **2** forms complementary base-paired duplexes independently from both triazole and t-amide faces. The triazole face duplexes A and B (Figure 3) result from new isomorphic bimodal PNA structure, in which the nucleobases are attached at C_α, quite different from that of standard PNA.

The designed bimodal PNA *bm*-PNA **2**, in the presence of DNA **1** and DNA **2** yielded the ternary complex DNA **2**:*bm*-PNA **2**:DNA **1** (Figure 3D) made from two duplexes. This complex showed a single melting transition (Figure 4b) with T_m of 56.6 °C, which is significantly higher than the constituent isolated duplexes DNA **2**:*bm*-PNA **2** and *bm*-PNA **2**:DNA **1** (Figure 5). The double duplex does not show a sequential melting (as in DNA triplexes[16]), but displays simultaneous dissociation of both DNA strands from *bm*-PNA **2** similar to PNA_2:DNA triplex.[2,17] The bimodal PNA backbone being common to both duplexes couples the unwinding of one duplex to influence that of other duplex, causing melting of both duplexes to be synchronous and not sequential. The coexistence of duplexes with common backbone in a single complex strengthens their mutual stability, impacting dissociation of both duplexes. These results provide proof of concept that as per the design, bimodal PNA concomitantly binds to two DNA strands that are complementary to triazole and t-amide face.

Creation of double duplex from *bm*-PNA **2**, DNA **1** and DNA **2** (Figure 3D) is a termolecular reaction requiring entropic cost. The two complementary DNA segments were connected by a tetranucleotide TTTT yielding single DNA $\mathbf{3}_{hp}$. This can now bind both sides to yield hairpin double duplex DNA $\mathbf{3}_{hp}$:*bm*-PNA **2** (Figure 3E) as a binary complex. This hairpin double duplex interestingly displayed two well-resolved transitions with T_m values of 34.6 and 65.4 °C (Figure 4c), in contrast to open double duplex that showed a single transition. The two transitions in hairpin duplex **3E** arise either from sequential melting of t-amide and triazole duplex, or the early transition from a premelting conformational change, followed by simultaneous disassociation of both strands. Notably, both observed transitions in hairpin duplex **3E** are stabilized, compared to isolated duplexes **3B** and **3C** and that of ternary complex **3D**. Note that in isolated duplexes and open double duplex **3D**, both duplexes are in antiparallel orientation. In hairpin double duplexes, the triazole duplex segment is in parallel orientation and hence stabilities are not directly comparable. The PNA:DNA transitions are generally known to be broad due to slow association−disassociation kinetics,[14] and in bimodal PNA duplex and double duplexes, they are even more broad.

The CD spectra of open double duplex **D** and hairpin double duplex **E** are shown in Figure 4d. The profiles resemble that observed for PNA:DNA duplexes,[18] indicating similar overall conformational features. Both **D** and **E** show a positive

https://dx.doi.org/10.1021/acs.orglett.0c01950
Org. Lett. XXXX, XXX, XXX−XXX

Table 1. Thermodynamic Parameters from ITC[a]

duplex	*bm*-PNA:DNA	$-\Delta G$ (kcal/mol)	$-\Delta H$ (kcal/mol)	$-\Delta S$ (cal/(mol K))	K_D ($\times 10^{-6}$ M)
B	*bm*-PNA **2**:DNA **1** (triazole)	6.67	33.7	94.0	8.78
C	DNA **2**:*bm*-PNA **2** (t-amide)	6.52	26.1	68.0	11.4
D	DNA **2**:*bm*-PNA **2**:DNA **1**	6.22	37.9	109.7	19.5
E	DNA $\mathbf{3}_{hp}$:*bm*-PNA **2**	7.49	24.8	60.0	2.11

[a]For experimental details, see Figures S10−S12 in the Supporting Information.

CD band at ∼280 nm, with a slight difference in negative band position: 260 nm for the open duplex **D** and 250 nm for hairpin duplex **E**. The CD band intensities were also higher for hairpin duplex **E**, compared to open duplex **D**, suggesting a better stacking in the hairpin duplex. The temperature-dependent CD of hairpin double duplex **E** (Figure S9 in the Supporting Information) showed slight shifts in maximum at 280 nm, accompanied by decreased intensity with an isosbestic point at ∼265 nm, indicating alteration in conformation during melting. The stacking of triazole rings concomitant with base pairing may provide additional stability in bimodal PNA duplexes. The results establish formation of double duplexes from *bm*-PNA **2** and biophysical mechanisms of melting of bimodal PNAs need further study.

The thermodynamic parameters for formation of duplexes and double duplexes in bimodal PNAs were sought from ITC (see Table 1, as well as Figures S10−S12 in the Supporting Information). The experiment with bimodal PNA double duplex **D** was performed by titrating an equimolar mixture (in terms of the number of bases/binding sites) of DNA **1** and DNA **2** into *bm*-PNA **2**. The dissociation constants (K_D) indicated the binding of triazole duplex **B** to be slightly stronger than t-amide duplex **C**, but association is entropically less favored (more negative). The stacking of triazole rings concomitant with canonical base pairing contributes to higher enthalpy, providing additional stability in the formation of *bm*-PNA **2** duplex **B**.

Formation of termolecular double duplex **D**, is accompanied by an entropic cost (more negative entropy), but offset by having a higher enthalpic contribution. Notably, the hairpin duplex **E** is most favored in terms of lowest K_D and lowest ($-\Delta S$) and highest ($-\Delta G$) among different complexes. The negative ΔG for bimodal PNA:DNA duplexes in the range of −6.0 kcal/mol to −7.0 kcal/mol was similar to that reported for PNA:DNA duplexes.[19]

In summary, this manuscript presents new concept of bimodal PNA that can concurrently hybridize with two cDNAs. In the isomorphic PNA backbone *iso*-PNA **1**, nucleobases anchoring on $C_\alpha(S)$ glycyl side chain successfully form triazole DNA duplex. The base pairing in this new isomorphic PNA duplex is likely to be Watson−Crick (WC) type, since it shows sequence specificity with lower T_m in mismatched duplex. The bimodal *bm*-PNA **2** designed to simultaneously bind two complementary DNAs forms open and hairpin double duplexes from t-amide and triazole faces. These coexist in a ternary complex with stability higher than the individual binary duplexes. The double duplex dissociates in a single step similar to PNA_2:DNA triplexes,[17] while the hairpin double duplex shows distinct premelting conformational change before disassociation.[16] This arises from the fact that a single common backbone hosts two duplexes. Based on choice of sequences (polypurines/polypyrimidines/self-complementary) on either side, bimodal PNAs can lead to fused duplexes, triplexes, and tetraplexes (G_n/C_n) with cDNA. They can be engineered to yield supramolecular functional nanostructures for probable applications in PNA material science.[20] Distant biotechnological applications include simultaneous targeting of two genes or micro RNA structures[21] for therapeutic purposes, and, as equivalents of short DNA staples, they can be active in programmed folding of plasmids in DNA origami.[22]

■ ASSOCIATED CONTENT

Supporting Information

The Supporting Information is available free of charge at https://pubs.acs.org/doi/10.1021/acs.orglett.0c01950.

Synthesis procedures, characterization data (NMR, MS of all new compounds, HPLC, MALDI TOF of PNA oligomers), UV-melting curves, CD spectra, ITC data (PDF)

■ AUTHOR INFORMATION

Corresponding Author

Krishna N. Ganesh − *Department of Chemistry, Indian Institute of Science Education and Research (IISER) Pune, Pune 411008, India; Department of Chemistry, Indian Institute of Science Education and Research (IISER) Tirupati, Tirupati 517507, India;* orcid.org/0000-0003-2292-643X; Email: kn.ganesh@iisertirupati.ac.in

Authors

Manoj Kumar Gupta − *Department of Chemistry, Indian Institute of Science Education and Research (IISER) Pune, Pune 411008, India*

Bharath Raj Madhanagopal − *Department of Chemistry, Indian Institute of Science Education and Research (IISER) Tirupati, Tirupati 517507, India;* orcid.org/0000-0003-1043-8754

Dhrubajyoti Datta − *Department of Chemistry, Indian Institute of Science Education and Research (IISER) Pune, Pune 411008, India*

Complete contact information is available at: https://pubs.acs.org/10.1021/acs.orglett.0c01950

Notes

The authors declare no competing financial interest.

■ ACKNOWLEDGMENTS

K.N.G. acknowledges the Department of Science and Technology (DST), New Delhi for a research grant (No. EMR/2016/007601). M.K.G. thanks UGC, New Delhi for a research fellowship. B.M. thanks IISER Tirupati, and D.D. thanks DST (Delhi) for postdoctoral fellowships.

REFERENCES

(1) Nielsen, P. E.; Egholm, M.; Berg, R. H.; Buchardt, O. Sequence selective recognition of DNA by strand displacement with thymine-substituted polyamide. *Science* **1991**, *254*, 1497−1500.

(2) Egholm, M.; Buchardt, O.; Nielsen, P. E.; Berg, R. H. Peptide Nucleic Acids (PNA). Oligonucleotide analogues with an achiral peptide backbone. *J. Am. Chem. Soc.* **1992**, *114*, 1895−1897.

(3) Egholm, M.; Nielsen, P. E.; Buchardt, O.; Berg, R. H. J. Recognition of guanine and adenine in DNA by cytosine and thymine containing peptide nucleic acids (PNA). *J. Am. Chem. Soc.* **1992**, *114*, 9677−9678.

(4) Egholm, M.; Buchardt, O.; Christensen, L.; Behrens, C.; Freier, S. M.; Driver, D. A.; Berg, R. H.; Kim, S. K.; Norden, B.; Nielsen, P. E. PNA hybridizes to complementary oligonucleotides obeying the Watson−Crick hydrogen-bonding rules. *Nature* **1993**, *365*, 566−568.

(5) (a) Nielsen, P. E.; Christensen, L. Strand displacement binding of a duplex forming homopurine PNA to a homopyrimidine duplex DNA target. *J. Am. Chem. Soc.* **1996**, *118*, 2287−2288. (b) Demidov, V. V.; Yavnilovich, M. V.; Belotserkovskii, B. P.; Frank-Kamenetskii, M. D.; Nielsen, P. E. Kinetics and mechanism of polyamide 'peptide' nucleic acid binding to duplex DNA. *Proc. Natl. Acad. Sci. U. S. A.* **1995**, *92*, 2637−2641.

(6) (a) Ray, A.; Norden, B. Peptide nucleic acid (PNA): its medical and biotechnical applications and promise for the future. *FASEB J.* **2000**, *14*, 1041−1060. (b) Nielsen, P. E. PNA technology. *Mol. Biotechnol.* **2004**, *26*, 233−248. (c) Lundin, K. E.; Good, L.; Stromberg, R.; Graslund, A.; Smith, C. I. E. Biological activity and biotechnological aspects of peptide nucleic acid. *Adv. Genet.* **2006**, *56*, 1−51. (d) D'Agata, R.; Giuffrida, M. C.; Spoto, G. Peptide nucleic acid-based biosensors for cancer diagnosis. *Molecules* **2017**, *22*, 1951−1966. (e) Vilaivan, T. Fluorogenic PNA probes. *Beilstein J. Org. Chem.* **2018**, *14*, 253−281. (f) Saarbach, J.; Sabale, P. M.; Winssinger, N. Peptide nucleic acid (PNA) and its applications in chemical biology, diagnostics and therapeutics. *Curr. Opin. Chem. Biol.* **2019**, *52*, 112−124. (g) Economos, N. G.; Oyaghire, S.; Quijano, E.; Ricciardi, A. S.; Saltzman, W. M.; Glazer, P. M. Peptide nucleic acids and gene editing: Perspectives on structure and repair. *Molecules* **2020**, *25*, 735−736.

(7) (a) Good, L.; Nielsen, P. E. Progress in developing PNA as a gene-targeted drug. *Antisense Nucleic Acid Drug Dev.* **1997**, *7*, 431−437. (b) Doyle, D. F.; Braasch, D. A.; Janowski, B. A.; Corey, D. R. Inhibition of gene expression inside cells by peptide nucleic acids: Effect of mRNA target sequence, mismatched bases, and PNA length. *Biochemistry* **2001**, *40*, 53−64. (c) Quijano, E.; Bahal, B.; Ricciardi, A.; Saltzman, W. M.; Glazer, P. M. Therapeutic peptide nucleic acids: Principles, limitations, and opportunities. *Yale J. Biol. Med.* **2017**, *90*, 583−598. (d) Montazersaheb, S.; Hejazi, M. S.; Charoudeh, H. N. Potential of peptide nucleic acids in future therapeutic applications. *Adv. Pharm. Bull.* **2018**, *8*, 551−563. (e) Lee, H. T.; Kim, S. K.; Yoon, J. W. Antisense peptide nucleic acids as a potential anti-infective agent. *J. Microbiol.* **2019**, *57*, 423−430. (f) Gambari, R.; Gasparello, J.; Finotti, A. Peptide nucleic acid-based targeting of microRNAs: possible therapeutic applications for glioblastoma. *J. Cancer Metastas. Treat.* **2019**, *5*, 55−62. (g) Smith, C. I. E.; Zain, R. Therapeutic oligonucleotides: State of the art. *Annu. Rev. Pharmacol. Toxicol.* **2019**, *59*, 605−630.

(8) (a) Hyrup, B.; Egholm, M.; Nielsen, P. E.; Wittung, P.; Norden, B.; Buchardt, O. Structure-activity studies of the binding of modified peptide nucleic acids (PNAs) to DNA. *J. Am. Chem. Soc.* **1994**, *116*, 7964−7970. (b) Kumar, V. A.; Ganesh, K. N. Conformationally constrained PNA analogues: Structural evolution toward DNA/RNA binding selectivity. *Acc. Chem. Res.* **2005**, *38*, 404−412. (c) Govindaraju, T.; Kumar, V. A.; Ganesh, K. N. (*SR/RS*)-Cyclohexanyl PNAs: Conformationally preorganized PNA analogues with unprecedented preference for duplex formation with RNA. *J. Am. Chem. Soc.* **2005**, *127*, 4144−4155. (d) Kumar, V. A.; Ganesh, K. N. Structure-editing of nucleic acids for selective targeting of RNA. *Curr. Top. Med. Chem.* **2007**, *7*, 715−726. (e) Corradini, R.; Sforza, S.; Tedeschi, T.; Totsingan, F.; Manicardi, A.; Marchelli, R. Peptide nucleic acids with a structurally biased backbone. Updated review and emerging challenges. *Curr. Top. Med. Chem.* **2011**, *11*, 1535−1554. (f) Moccia, M.; Adamo, M. F. A.; Saviano, M. Insights on chiral, backbone modified peptide nucleic acids: Properties and biological activity. *Artif. DNA PNA XNA* **2014**, *5*, e1107176.

(9) (a) Koppelhus, U.; Nielsen, P. E. Cellular delivery of peptide nucleic acid (PNA). *Adv. Drug Delivery Rev.* **2003**, *55*, 267−280. (b) Równicki, M.; Wojciechowska, M.; Wierzba, A. J.; Czarnecki, J.; Bartosik, D.; Gryko, D.; Trylska, J. Vitamin B12 as a carrier of peptide nucleic acid (PNA) into bacterial cells. *Sci. Rep.* **2017**, *7*, 7644. (c) Gasparello, J.; Manicardi, A.; Casnati, A.; Corradini, R.; Gambari, R.; Finotti, A.; Sansone, F. Efficient cell penetration and delivery of peptide nucleic acids by an argininocalix[4]arene. *Sci. Rep.* **2019**, *9*, 3036−3045.

(10) (a) Mitra, R.; Ganesh, K. N. PNAs grafted with (α/γ, *R/S*)-aminomethylene pendants: Regio and stereospecific effects on DNA binding and improved cell uptake. *Chem. Commun.* **2011**, *47*, 1198−1200. (b) Mitra, R.; Ganesh, K. N. Aminomethylene peptide nucleic acid (*am*-PNA): synthesis, regio-/ stereospecific DNA binding, and differential cell uptake of (α/γ, *R/S*) am-PNA analogues. *J. Org. Chem.* **2012**, *77*, 5696−5704. (c) Jain, D. R.; Anandi V, L.; Lahiri, M.; Ganesh, K. N. Influence of pendant chiral Cγ-(alkylideneamino/guanidino) cationic side-chains of PNA backbone on hybridization with complementary DNA/RNA and cell permeability. *J. Org. Chem.* **2014**, *79*, 9567−9577. (d) Ellipilli, S.; Palvai, S.; Ganesh, K. N. Fluorinated peptide nucleic acids with fluoroacetyl side chain bearing 5-(F/CF_3)-uracil: Synthesis and cell uptake studies. *J. Org. Chem.* **2016**, *81*, 6364−6373. (e) Ellipilli, S.; Vasudeva Murthy, R.; Ganesh, K. N. Perfluoroalkylchain conjugation as a new tactic for enhancing cell permeability of peptide nucleic acids (PNAs) via reducing the nanoparticle size. *Chem. Commun.* **2016**, *52*, 521−524.

(11) (a) Dragulescu-Andrasi, A.; Rapireddy, S.; Frezza, B. M.; Gayathri, C.; Gil, R. R.; Ly, D. H. A simple gamma-backbone modification preorganizes peptide nucleic acid into a helical structure. *J. Am. Chem. Soc.* **2006**, *128*, 10258−10267. (b) Ishizuka, T.; Yoshida, J.; Yamamoto, Y.; Sumaoka, J.; Tedeschi, T.; Corradini, R.; Sforza, S.; Komiyama, M. Chiral introduction of positive charges to PNA for double-duplex invasion to versatile sequences. *Nucleic Acids Res.* **2008**, *36*, 1464−1471.

(12) (a) Branda, N.; Kurz, G.; Lehn, J.-M. Janus wedges: A new approach towards nucleobase-pair recognition. *Chem. Commun.* **1996**, 2443−2444. (b) Zhao, H.; Huang, W.; Wu, X.; Qing, Y.; Xing, Z.; He, Y. Synthesis of a complete Janus-type guanosine-cytosine base and its 2'-deoxyribonucleoside. *Chem. Lett.* **2011**, *40*, 684−686. (c) Chen, H.; Meena; McLaughlin, L. M. A Janus-wedge DNA triplex with A-W1-T and G-W2-C base triplets. *J. Am. Chem. Soc.* **2008**, *130*, 13190−13191. (d) Shin, D.; Tor, Y. Bifacial nucleoside as a surrogate for both T and A in duplex DNA. *J. Am. Chem. Soc.* **2011**, *133*, 6926−6929. (e) Artigas, G.; Marchan, V. Synthesis of Janus compounds for the recognition of G-U mismatched nucleobase pairs. *J. Org. Chem.* **2013**, *78*, 10666−10677.

(13) (a) Xia, X.; Piao, X.; Bong, D. Bifacial peptide nucleic acid as an allosteric switch for aptamer and ribozyme function. *J. Am. Chem. Soc.* **2014**, *136*, 7265−7268. (b) Thadke, S. A.; Hridya, V. M.; Perera, J. D. R.; Gil, R. R.; Mukherjee, A.; Ly, D. H. Shape selective bifacial recognition of double helical DNA. *Comm. Chem.* **2018**, *1*, 79. (c) Thadke, S. A.; et al. Design of bivalent nucleic acid ligands for recognition of RNA-repeated expansion associated with Huntington's disease. *Biochemistry* **2018**, *57*, 2094−2108.

(14) (a) Bentin, T.; Hansen, G. I.; Nielsen, P. E. Measurement of PNA binding to double-stranded DNA. In *Methods in Molecular Biology*; Nielsen, P. E., Ed.; Humana Press: Totowa, NJ, 2002; *Vol. 208*, pp 91−109. (b) Nielsen, P. E., Ed. *Peptide Nucleic Acids Protocols and Applications*, 2nd Edition; Horizon Bioscience: Norfolk, U.K., 2004.

(15) (a) Sen, A.; Nielsen, P. E. Unique properties of purine/pyrimidine asymmetric PNA-DNA duplexes: Differential stabilization of PNA-DNA duplexes by purines in the PNA strand. *Biophys. J.* **2006**, *90*, 1329−1337. (b) Jasiński, M.; Miszkiewicz, J.; Feig, M.;

https://dx.doi.org/10.1021/acs.orglett.0c01950
Org. Lett. XXXX, XXX, XXX−XXX

Trylska, J. Thermal stability of peptide nucleic acid complexes. *J. Phys. Chem. B* **2019**, *123*, 8168−8177.
(16) Plum, D. E.; Park, Y.-W.; Singleton, S. F.; Dervan, P. B.; Breslauer, K. J. Thermodynamic characterization of the stability and the melting behavior of a DNA triplex: A spectroscopic and calorimetric study. *Proc. Natl. Acad. Sci. U. S. A.* **1990**, *87*, 9436−9440.
(17) Krupnik, O. V.; Guscho, Y. A.; Sluchanko, K. A.; Nielsen, P. E.; Lazurkin, Y. S. Thermodynamics of the melting of PNA_2/DNA triple helices. *J. Biomol. Struct. Dyn.* **2001**, *19*, 535−542.
(18) Corradini, R.; Tedeschi, T.; Sforza, S.; Marchelli, R. Electronic Circular Dichroism of Peptide Nucleic Acids and Their Analogues. In *Comprehensive Chiroptical Spectroscopy, Vol. 2: Applications in Stereochemical Analysis of Synthetic Compounds, Natural Products, and Biomolecules*; Berova, N., Polavarapu, P. L., Nakanishi, K., Woody, R. W., Eds.; John Wiley & Sons, Inc, 2012; pp 581−617.
(19) Ratilainen, T.; Holmen, A.; Tuite, E.; Nielsen, P. E.; Norden, B. Thermodynamics of sequence-specific binding of PNA to DNA. *Biochemistry* **2000**, *39*, 7781−7791.
(20) (a) Manicardi, A.; Rozzi, A.; Korom, S.; Corradini, R. Building on the peptide nucleic acid (PNA) scaffold: a biomolecular engineering approach. *Supramol. Chem.* **2017**, *29*, 784−795. (b) Duan, T.; He, L.; Tokura, Y.; Liu, X.; Wu, Y.; Shi, Z. Construction of tunable peptide nucleic acid junctions. *Chem. Commun.* **2018**, *54*, 2846−2850. (c) Swenson, C. S.; Velusamy, A.; Argueta-Gonzalez, H. S.; Heemstra, J. Bilingual peptide nucleic Acids: Encoding the languages of nucleic acids and proteins in a single self-assembling biopolymer. *J. Am. Chem. Soc.* **2019**, *141*, 19038−19047. (d) Canady, T. D.; Berlyoung, A. S.; Martinez, J. A.; Emanuelson, C.; Telmer, C. A.; Bruchez, M. P.; Armitage, B. A. Enhanced hybridization selectivity using structured gamma PNA probes. *Molecules* **2020**, *25*, 970−982.
(21) Cadoni, E.; Manicardi, A.; Madder, A. PNA-based microRNA detection methodologies. *Molecules* **2020**, *25*, 1296−1321.
(22) (a) Hong, F.; Zhang, F.; Liu, Y.; Yan, H. DNA Origami: Scaffolds for creating higher order structures. *Chem. Rev.* **2017**, *117*, 12584−12640. (b) Bila, H.; Kurisinkal, E. E.; Bastings, M. M. C. Engineering a stable future for DNA-origami as a biomaterial. *Biomater. Sci.* **2019**, *7*, 532−541.

https://dx.doi.org/10.1021/acs.orglett.0c01950
Org. Lett. XXXX, XXX, XXX−XXX